

# Effect of Doped Substrate on GaAs–AlGaAs Interfacial Workfunction IR Detector Response Through Cavity Effect

Steven G. Matsik, Mohamed B. M. Rinzan, Dmitriy G. Esaev, A. G. Unil Perera, *Senior Member, IEEE*, G. von Winckel, Andreas Stintz, Sanjay Krishna, H. C. Liu, M. D. Byloos, T. Oogarah, G. I. Sproule, K. Liu, and M. Buchanan

**Abstract**—In this paper, results are reported showing response enhancement in GaAs–AlGaAs IR detectors using a doped substrate to increase reflection, enhancing the resonant cavity effect. Responsivity for heterojunction interfacial workfunction detectors grown on semi-insulating (SI) and doped substrates are compared. For a device grown on an SI substrate, a 9- $\mu\text{m}$  resonance peak had a response of 1.5 mA/W while a similar device on an n-doped substrate showed 12 mA/W. Also, the difference between response under forward and reverse bias (3 versus 12 mA/W) for the sample grown on the doped substrate, as well as calculated results confirm that the increased response is due to the resonant enhancement. An optimized design for a 15- $\mu\text{m}$  peak (24  $\mu\text{m}$  0 response threshold) detector grown on a doped substrate could expect a peak response of 4 A/W with a 50% quantum efficiency and  $D^* \sim 2 \times 10^{10}$  Jones at the background limited temperature of 50 K.

**Index Terms**—GaAs–AlGaAs, heterojunctions, IR detectors.

## I. INTRODUCTION

RECENT developments in the application of infrared sources such as the transmission of digital signals using lasers with  $\lambda$  in the range 7–10  $\mu\text{m}$  [1] have generated renewed interest in detectors operating in the 5–20  $\mu\text{m}$ -range. The development of quantum cascade (QC) lasers operating at 21.5 and 24  $\mu\text{m}$  [2] will extend the range of interest in these applications to longer wavelengths, requiring fast detectors operating at wavelengths longer than the currently available [3] ( $\sim 20 \mu\text{m}$ ) HgCdTe and quantum well infrared photodetectors (QWIPs). The spectral lines in this range from many gases make IR detectors in this range important for applications in gas detection and identification systems, such as pollution monitoring on Earth and for astronomical study of gas or dust clouds [4], [5].

Resonant cavity effects have been used to enhance response in many devices [6] including QWIPs [7] photodiodes, photo-

Manuscript received July 21, 2004; revised November 29, 2004. This work was supported in part by the NSF under Grant ECS-0140434 and in part by the DOE/BES under grant DE-FG03-02ER46014. The work at the National Research Council is supported in part by DND. M. B. M. Rinzan is supported by GSU RPE funds. The review of this paper was arranged by Editor K. Najafi.

S. G. Matsik, M. B. M. Rinzan, D. G. Esaev, and A. G. U. Perera are with the Department of Physics and Astronomy, Georgia State University, Atlanta, GA 30303 USA.

G. von Winckel, A. Stintz, and S. Krishna are with the Center for High Technology Materials, University of New Mexico, Albuquerque, NM 87106 USA.

H. C. Liu, M. D. Byloos, T. Oogarah, G. I. Sproule, K. Liu, and M. Buchanan are with the Institute for Microstructural Sciences, National Research Council, Ottawa, ON K1A 0R6, Canada.

Digital Object Identifier 10.1109/TED.2005.843876

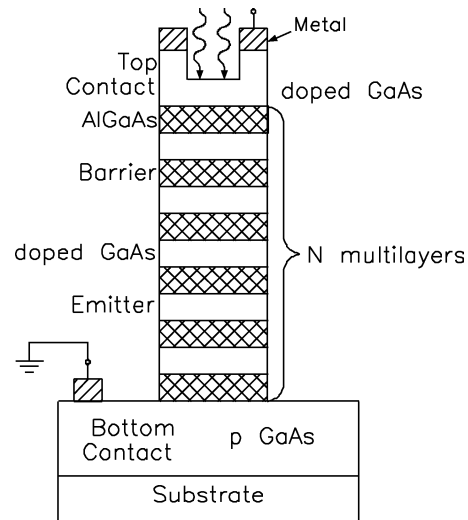


Fig. 1. Structure of the detector after processing showing the layers of the device. Absorption occurs in the doped GaAs emitters with photoemission over the undoped AlGaAs barriers. The layer parameters are given in Table I.

transistors, modulators, and LEDs. In this paper, results are presented on increasing the detector response in the 5–20  $\mu\text{m}$  region through the use of doped substrates to improve the enhancement from reflection. The top surface will be an antinode with the bottom surface a node. In this configuration  $\sim 30\%$  of the light which enters the device will contribute to multiple reflections.

## II. RESONANT CAVITY EFFECT

The development of GaAs–AlGaAs heterojunction interfacial workfunction internal photoemission (HEIWIP) detectors has demonstrated devices with 0 response threshold wavelengths ( $\lambda_0$ ) ranging from 15 to 92  $\mu\text{m}$  [8]. The basic detection process [9] in a HEIWIP detector is by free carrier absorption in the heavily doped emitter region, internal photoemission [10] over the workfunction at the emitter/barrier interface and then sweep out and collection of the excited carriers. The standard approach uses GaAs emitters and  $\text{Al}_x\text{Ga}_{1-x}\text{As}$  barriers (see Fig. 1 for a device structure.) The prime alternative for the 20–40  $\mu\text{m}$  range are the Si BIB detectors which use photoexcitation of carriers from the impurity band to the conduction band. HEIWIPs do not need to keep the impurity band separate, hence much higher doping leading to higher absorption are

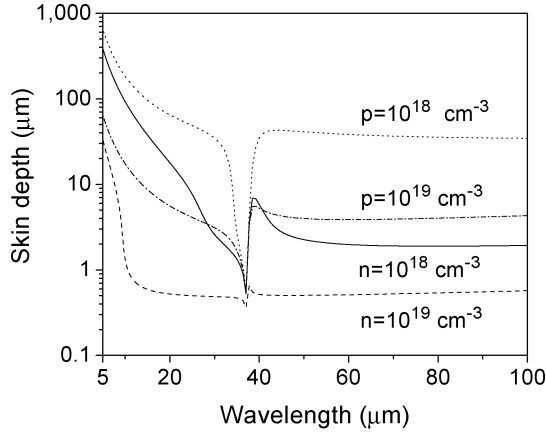


Fig. 2. Skin depth for infrared radiation in GaAs with both n- and p-type doping of  $10^{18}$  and  $10^{19}$   $\text{cm}^{-3}$ . The skin depth is relatively constant at long wavelengths and increases rapidly at short wavelengths. The feature between 35 and 40  $\mu\text{m}$  is due to the reststrahlen effect. Skin depth is least for n-type material.

possible. Thickness of the structure was used previously to increase the resonant cavity enhancement (RCE) [11]. Here results are reported on the use of doped substrates for RCE in the device. The idea of the resonant cavity architecture is to use the reflection from the bottom surface to provide a standing wave in the device. Placing the emitters at the antinodes in the resulting resonant cavity structure will increase absorption and enhance the response at the resonant wavelengths. RCE effects have already been demonstrated in the reflection, transmission and absorption of structures with semi-insulating substrates [12]. The next step is to demonstrate increased detector response from the RCE due to the doped substrate.

One of the requirements for using RCE in HEIWIP devices is a high reflection from the bottom of the device structure in order to achieve a standing wave. Since the substrates used are typically 400–600  $\mu\text{m}$  thick, the reflection from the bottom of an undoped substrate cannot be used to form low order resonances in the 1–50- $\mu\text{m}$  response range. Two possible approaches to developing a usable resonant cavity architecture in devices are 1) to use a doped substrate as the reflector or; 2) to grow a reflecting structure below the active region of the device. The reflecting structure could be as simple as a single doped layer or could involve multiple doped and undoped layers as in a Bragg reflector [13]. In some cases the bottom contact could also be the reflector, or the reflector may be grown separately. Here results are reported on the use of the first approach, i.e., the device grown on an n-type substrate.

The effectiveness of a reflecting layer depends on its thickness and the skin depth  $\delta$ . For layers with thickness less than  $3\delta$ , a significant fraction of the radiation will be transmitted rather than reflected. The results of skin depth calculated from the complex dielectric constant derived as in [8] for both n- and p-type materials are shown in Fig. 2. For longer wavelengths ( $> 40$   $\mu\text{m}$ ) the skin depth stays relatively constant with values between  $\sim 40$   $\mu\text{m}$  for p-type material doped to  $10^{18}$   $\text{cm}^{-3}$  and 0.6  $\mu\text{m}$  for n-type material doped to  $10^{19}$   $\text{cm}^{-3}$ . As the wavelength is decreased, the skin depth increases, becoming larger than 100  $\mu\text{m}$  at wavelengths shorter than 10  $\mu\text{m}$  for p-type doping. The sharp drop in skin depth observed at 35–40  $\mu\text{m}$  is due to the reststrahlen effect. The lower effective mass for

electrons compared to holes leads to the reduced skin depth in n-type material. Although reflection is improved by the use of n-doping, a device based totally on n-type material is not optimum for IR detection. For lower carrier mass, the absorption coefficient will increase, however, the increased Fermi level will greatly reduce photoemission. The relative magnitude of these two effects will depend on the doping in the emitters. For low doping levels the lighter carriers will be more efficient while at higher doping heavier carriers will be more efficient. At the doping levels in the devices to be reported here ( $\sim 3 \times 10^{17}$   $\text{cm}^{-3}$ ) the efficiency of n-type emitter material is about 0.95 times the efficiency for p-type. As the experimental results indicate that higher doping than those used here are desirable, the optimum design should use an n-type reflecting layer at the bottom with p-type emitters to enhance photoresponse.

For a typical HEIWIP device, p-doped  $\sim 10^{19}$ - $\text{cm}^{-3}$ , 0.7- $\mu\text{m}$ -thick bottom contacts are grown [8]. This is less than the skin depth at all wavelengths. Hence, a significant fraction of the incident radiation will pass through the bottom contact rather than being reflected, reducing the strength of the resonance amplitude. Even for highly n-doped material this is only similar to the skin depth at long wavelengths ( $> 10$   $\mu\text{m}$  for  $1 \times 10^{19}$   $\text{cm}^{-3}$  n-type material). By increasing the reflecting layer thickness to  $\sim 1.5$   $\mu\text{m}$  for n-type material an effective cavity could be formed at  $\lambda > 10$   $\mu\text{m}$ . However, for shorter wavelengths, growing a thick enough reflecting layer will not be feasible due to the larger skin depth. The skin depth limitation is responsible for the difficulty in clearly identifying resonance maxima in previous p-type HEIWIPs [9]. One solution to the difficulty is to use a doped substrate to provide the reflecting layer. A doped substrate should increase the reflection from the substrate near the active region without the need to grow a thick reflecting layer. The use of a doped substrate will increase the doped layer thickness to several skin depths, leading to minimal transmission through the substrate and hence increased reflection.

The device response can be modeled using

$$R = \frac{q\eta}{hf} \quad (1)$$

where  $q$  is the electron charge,  $\eta$  is the total quantum efficiency of the detector,  $f$  is the frequency, and  $h$  is Planck's constant. The total quantum efficiency is the product of the photon absorption efficiency and the internal quantum efficiency (the probability that photoexcited carriers undergo internal photoemission)  $\eta = \eta_a \eta_i$ . Here, the collection efficiency is assumed to be 1 since the maximum barrier height is at the interface due to the absence of space charge effects so that any carriers scattered after internal photoemission will be collected. The absorption efficiency can be determined from the imaginary part of the complex dielectric constant given in the Drude model by

$$\epsilon_j(\omega) = \epsilon_{\infty,j} \left[ 1 - \frac{\omega_{p,j}^2}{\omega(\omega + i\omega_{0,j})} \right] + \frac{\omega_{TO,j}^2(\epsilon_{s,j} - \epsilon_{\infty,j})}{\omega_{TO,j}^2 - \omega^2 - i\omega\gamma_j} \quad (2)$$

The optical field strength in the layers can be determined from matching the field at the layer interfaces [11]. The internal efficiency is found from an escape cone model [10] and is the fraction of carriers with energy associated with motion perpendicular to the layers greater than the barrier energy.

TABLE I

DEVICE PARAMETERS FOR THE TWO DEVICES USED TO DEMONSTRATE THE RESONANT CAVITY EFFECT. THE DEVICES WERE THE SAME EXCEPT FOR HE0205 BEING p-DOPED AND GROWN ON AN SI SUBSTRATE WHILE 1329 IS n-TYPE AND GROWN ON AN n-TYPE SUBSTRATE WITH DOPING  $\sim 5 \times 10^{18} \text{ cm}^{-3}$

Sample	Emitter Doping ( $10^{17} \text{ cm}^{-3}$ )	Emitter Thickness ( $\text{\AA}$ )	Barrier Thickness ( $\text{\AA}$ )	Number of Layers	Contact Doping ( $10^{18} \text{ cm}^{-3}$ )	Peak Response (mA/W)	Doping & Substrate
HE0205	3	188	1250	12	10	1.5	p, SI
1329	4	188	1250	12	1	12	n, n

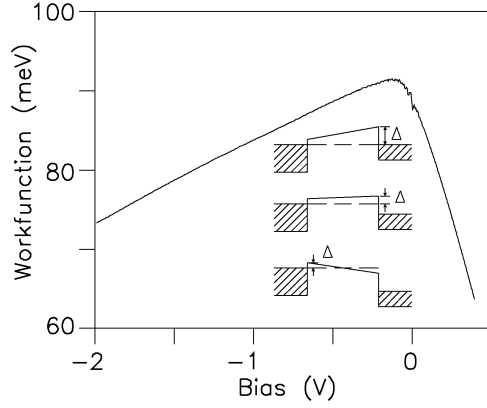


Fig. 3. Experimental variation in the workfunction with the bias for sample 1329 with a doped substrate. There is a rapid drop for forward bias and a slow drop for reverse bias. The inset shows a band diagram of the first barrier with the contact on the left and an emitter on the right. The higher doping in the contact gives a higher Fermi level. Under 0 bias (top diagram) the barrier slopes up with the highest value adjacent to the emitter. Under low bias (middle diagram) the barrier slopes up with the effective barrier height  $\Delta$  reduced by the applied bias. Under high bias (bottom diagram) the barrier slopes down and  $\Delta$  is determined from the contact and has only a slow variation with bias.

### III. EXPERIMENT

Two GaAs–AlGaAs samples 1329 with a doped substrate and HE0205 with an intrinsic substrate were used to demonstrate the resonant cavity enhancement from the doped substrate. The parameters for the two devices are given in Table I. The significant difference between the samples was the use of an SI substrate in HE0205 and an n-type substrate in 1329. Both devices used GaAs emitters and  $\text{Al}_{0.15}\text{Ga}_{0.85}\text{As}$  barriers. However, HE0205 had p-doped emitters while 1329 had n-doped emitters. From calculations using the model of [11] it is expected that n-type emitters will be 95% as efficient as p-doped emitters. Hence, even the small difference expected for the n-type layers will reduce the response. Thus, the increase observed in the response should be due to cavity effects.

The dark current for both devices were measured and a significant feature was a rapid decrease in the barrier height  $\Delta$ , determined from Arrhenius plots, observed for 1329 under forward bias and a slower decrease under reverse bias as shown in Fig. 3. Typically,  $\Delta$  is expected to vary about 10 meV at these doping levels, while for 1329 it decreases from 95 to 45 meV as the bias is varied from 0 to 0.7 V. This variation is believed to be due to the difference in doping in the contact and emitter layers and could be used to tune  $\lambda_0$  by varying the bias. The doping in the contact layer is  $2 \times 10^{18} \text{ cm}^{-3}$  giving a much higher Fermi level than in the emitters which were doped to  $4 \times 10^{17} \text{ cm}^{-3}$ . The difference in the Fermi levels will lead to band bending in

the first barrier layer with a result that the conduction band edge under 0 bias increases from the contact toward the emitter as seen in the top inset in Fig. 3. The effective barrier height is determined by the difference between the Fermi level and the maximum height of the barrier. When a bias is applied to the device the effective barrier height can be determined from an Arrhenius plot of  $\ln(I/T^{3/2})$  versus  $1/T$ . Under a small bias (middle inset in Fig. 3) the highest energy for the conduction band will still be adjacent to the emitter. However, it will be reduced due to the applied field in the barrier and bias dependence of the barrier will be observed. Above a certain bias, the drop due to the applied field will exceed the effects of the band bending and the barrier will slope down from the contact to the emitter (bottom inset in Fig. 3). The effective barrier is now determined by the barrier height adjacent to the contact which will then vary only slowly with bias. The difference in behavior for forward and reverse bias is probably related to small differences between the doping in the two contacts. The fact that the variation is seen only in the forward and not in the reverse direction means that a large difference in  $\lambda_0$  will be seen between the forward and reverse directions. Because of this  $\lambda_0$  variation, comparison of response in the forward and reverse directions will have to be limited (to less than the peak wavelength) to obtain valid results. When the resonant cavity effect is ignored as seen in [8], the response increases linearly with the wavelength for short wavelengths, reaching a maximum, and then decreases to 0 at  $\lambda_0$ . Previous results [8] (both calculated and experimental) for samples with different  $\lambda_0$  have shown that for the short wavelength region where response increases linearly, the response does not depend on the  $\lambda_0$ . However, for longer wavelengths response increases as  $\lambda_0$  is increased. By restricting the comparison to the linear region ( $< 10 \mu\text{m}$  for sample 1329), the difference in  $\lambda_0$  between forward and reverse bias can be ignored.

The contacts can also serve as emitters for the devices and can make a significant contribution to the device response. For HE0205 the contact doping is  $1 \times 10^{19} \text{ cm}^{-3}$  while the emitters are only doped to  $3 \times 10^{17}$ . Based on the device model, response from the top contact should be almost ten times the response from the emitters and 30 times the response from the bottom contact. The forward bias response for HE0205 with a peak response of 1.5 mA/W is shown in Fig. 4, while reverse bias response was not measurable. The two key properties of this sample are the use of an SI substrate and p-type doping. Any reflection in the undoped substrate structure must come from the bottom contact. This means that the optical electric field and hence the absorption should be small in the bottom contact compared to the top contact as was observed experimentally. For a p-type device, forward bias causes the top contact to

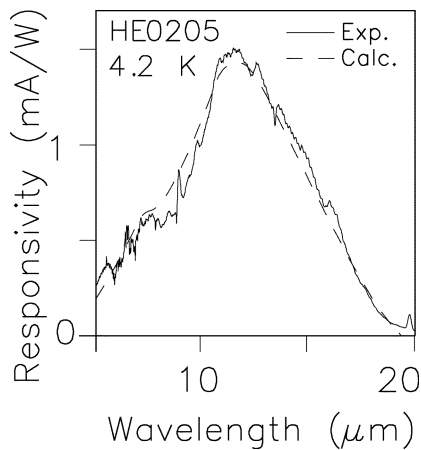


Fig. 4. Response under forward bias for the HE0205 sample at 4.2 K. Response was not observed under reverse bias. The dashed line shows the modeled response for the same detector parameters.

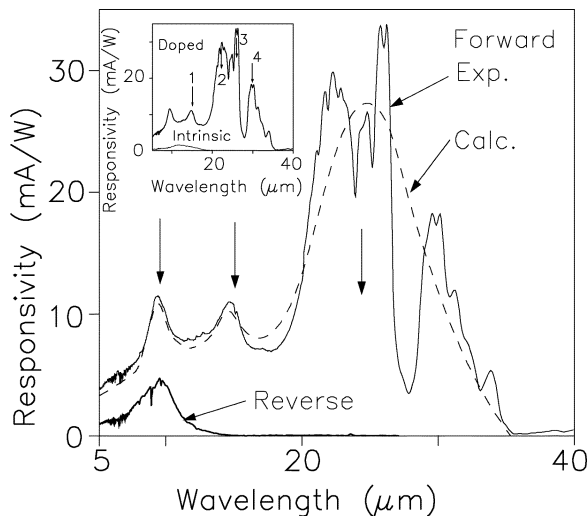


Fig. 5. Response under forward and reverse bias for the sample 1329 (grown on an n-type substrate) at 4.2 K. The response is much stronger under forward bias than reverse bias. The peak at  $10 \mu\text{m}$  is enhanced by waveguide effects under the contact region. The numbered peaks correspond to minima in the reflectance shown in Fig. 6. The dashed line shows the modeled response for the same detector parameters. The inset shows a comparison of the response for the doped and intrinsic substrate samples.

serve as an emitter with a strong response and reverse bias causes the bottom contact to serve as the emitter with weak or no response.

The response under forward and reverse bias for sample 1329 is shown in Fig. 5. Response was seen for both cases, although the forward bias signal of  $12 \text{ mA/W}$  at  $9 \mu\text{m}$  was a factor of four stronger than the reverse bias signal of  $3 \text{ mA/W}$ . The comparison was done at  $9 \mu\text{m}$  so that the difference in  $\lambda_0$  for forward and reverse bias should not affect the responsivity. Again, the observed characteristics of the response are consistent with the resonant cavity enhancement. Sample 1329 was grown on an n-doped substrate for which the reflection will occur inside the substrate at a point near the skin depth from the substrate/contact interface.

This means that absorption will occur in both the top and bottom contacts. Under forward bias three peaks are seen corre-

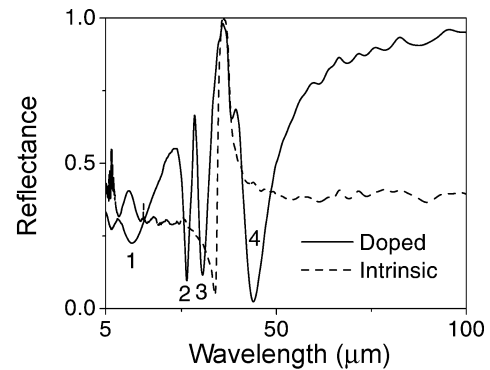


Fig. 6. Reflectance measurements for both samples showing an increased reflection from sample 1329 as well as the reduced reflection (labeled 1–4) corresponding to response peaks labeled in Fig. 5.

sponding to the  $\lambda/4$ ,  $3\lambda/4$ , and  $5\lambda/4$  cavity resonances. Since the skin depth varies with wavelength, the effective thickness of the cavity will also vary with wavelength, and the observed peaks do not have frequencies that are multiples of the fundamental. When resonances are fitted using a basic model for the HEIWP response [8] with the absorption calculated from the resonant cavity effect as was done previously [11], and a gain of 2.0, a good agreement with the experimental values are seen as indicated in Figs. 4 and 5. The fit for the reverse bias response for sample 1329 matches the experimental curve but is not shown for simplicity. To obtain the fit the workfunction for the contact was assumed to be the value obtained from the Arrhenius plots while the workfunction for the emitters were taken as the  $90 \text{ meV}$  calculated from the design parameters. The difference in workfunctions introduces a threshold for the emitters just longer than the  $5\lambda/4$  resonance peak leading to enhancement of the peak.

A comparison of the response of the two samples under forward bias indicates the presence of a resonant cavity enhancement in sample 1329, which was eight times the response for the HE0205 sample with the SI substrate as seen in the inset to Fig. 5. This is due to the efficient cavity formation caused by the reflection from the doped substrate. The increased resonant cavity nature can also be seen in the reflection measurements given in Fig. 6. For sample 1329 the average reflection is much higher than for the intrinsic substrate sample. The reduced reflection at the resonances (reflection minima indicated by 1–4) match the response peaks indicated by the arrows labeled 1–4 in the inset to Fig. 5. The unlabeled response maximum at  $10 \mu\text{m}$  does not appear in the absorption as it is believed to be related to the metallization on the detector which is not present on the absorption sample. The light which is reflected under the metal contact undergoes resonance at both the top and bottom of the device with a resonance at  $\sim 10 \mu\text{m}$ . The differences predicted by the model for p- and n-emitters with a SI substrate and for n-emitters with an n-substrate are shown in Fig. 7. The change in emitter type has only a minimal effect on the response while the n-substrate produces a large increase.

These results can be used to optimize a detector operating in the  $12\text{--}20\text{-}\mu\text{m}$  range. The doping in the emitters of the measured devices was only  $3 \times 10^{17} \text{ cm}^{-3}$ . By increasing the doping to  $3 \times 10^{18} \text{ cm}^{-3}$  in the emitters so that response from the emitters

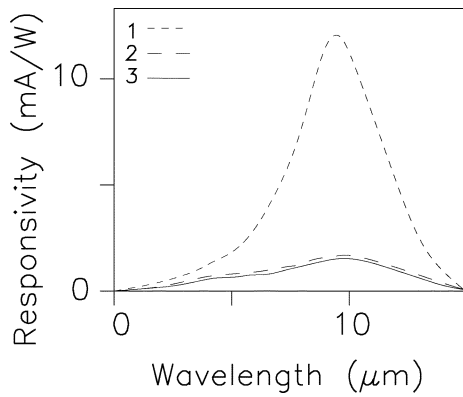


Fig. 7. Difference in calculated response for devices with (1) n-type emitters grown on an n-substrate and (2) n and (3) p-type emitters grown on an SI substrate. The device parameters are the same as for HE0205. The change from p- to n-emitters produces only a minimal change while the use of an n-substrate produces an increase of  $\sim 8$  times in the response.

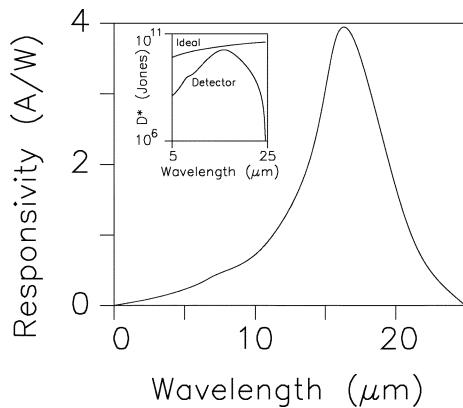


Fig. 8. Response for an optimized device with 32 periods of 200 Å GaAs emitters p-doped to  $3 \times 10^{18} \text{ cm}^{-3}$  and 350 Å  $\text{Al}_{0.15}\text{Ga}_{0.85}\text{As}$  barriers using an n-substrate with doping  $5 \times 10^{18} \text{ cm}^{-3}$ . The responsivity has been increased to near 4 A/W. The inset shows the calculated  $D^*$  value with a peak value of  $\sim 2 \times 10^{10}$  Jones as well as the calculated result for an ideal detector.

is similar to the contacts, a device with improved response can be obtained. An n-substrate would be used to provide maximum resonant cavity enhancement. Hence, a HEIWIP detector with 32 periods of 200 Å GaAs emitters p-doped to  $3 \times 10^{18} \text{ cm}^{-3}$  and 350 Å  $\text{Al}_{0.15}\text{Ga}_{0.85}\text{As}$  barriers using an n-substrate should be near optimum for operation in the range 12–20  $\mu\text{m}$  with a threshold near 24  $\mu\text{m}$ . The responsivity of such a device as shown in Fig. 8 should be near 4 A/W with a total quantum efficiency of 50% and  $D^* \sim 2 \times 10^{10}$  Jones at 77 K and a background limited temperature of 50 K.

#### IV. CONCLUSION

Enhanced resonant cavity effects have been demonstrated from the use of doped substrates in HEIWIP detectors. A sample with a doped substrate showed a factor of 8 increase from 1.5 to 12 mA/W over a sample on an undoped substrate. The difference (3 mA/W compared to 12 mA/W) between response from the top and bottom contacts gives additional indication that the enhanced response is due to resonant cavity

effects. This demonstration of improved response from use of a doped substrate offers possibilities of improving response in HEIWIP detectors.

#### REFERENCES

- [1] F. Capasso *et al.*, "Quantum cascade lasers: ultrahigh-speed operation, optical wireless communication, narrow linewidth, and far-infrared emission," *IEEE J. Quantum Electron.*, vol. 38, no. 5, pp. 511–532, May 2002.
- [2] R. Colombelli, F. Capasso, C. Gmachl, A. L. Hutchinson, D. L. Sivco, A. Tredicucci, M. C. Wanke, A. M. Sergent, and A. Y. Cho, *Appl. Phys. Lett.*, vol. 78, pp. 2620–2622, 2001.
- [3] A. G. U. Perera, H. C. Liu, and M. H. Francombe, Eds., *Handbook of Thin Film Devices: Semiconductor Optical and Electrooptical Devices*. New York: Academic, 2001.
- [4] P. Garcia-Lario *et al.*, *Astrophys. J.*, vol. 513, pp. 941–946, 1999.
- [5] H. Izumura *et al.*, *Astron. Astrophys.*, vol. 315, pp. L221–L224, 1996.
- [6] M. S. Unlu, G. Ulu, and M. Gokkavas, "Resonant cavity enhanced photodetectors," in *Photodetectors and Fiber Optics*, H. S. Nalwa, Ed. New York: Academic, 2001, pp. 97–201.
- [7] A. Shen, H. C. Liu, M. Gao, E. Dupont, M. Buchanan, J. Ehret, G. J. Brown, and F. Szmulowicz, *Appl. Phys. Lett.*, vol. 77, pp. 2400–2402, 2000.
- [8] S. G. Matsik, M. B. M. Rinzan, A. G. U. Perera, H. C. Liu, Z. R. Wasilewski, and M. Buchanan, *Appl. Phys. Lett.*, vol. 82, pp. 139–141, 2003.
- [9] A. G. U. Perera, S. G. Matsik, B. Yaldiz, H. C. Liu, A. Shen, M. Gao, Z. R. Wasilewski, and M. Buchanan, *Appl. Phys. Lett.*, vol. 78, pp. 2241–2243, 2001.
- [10] A. G. U. Perera, H. X. Yuan, and M. H. Francombe, *J. Appl. Phys.*, vol. 77, pp. 915–924, 1995.
- [11] D. G. Esaeu, S. G. Matsik, M. B. M. Rinzan, A. G. U. Perera, H. C. Liu, and M. Buchanan, *J. Appl. Phys.*, vol. 93, pp. 1879–1883, 2003.
- [12] A. L. Korotkov, A. G. U. Perera, W. Z. Shen, J. Herfort, K. H. Ploog, W. J. Schaff, and H. C. Liu, *J. Appl. Phys.*, vol. 89, pp. 3295–3300, 2001.
- [13] J. P. van der Ziel and M. Ilegens, *Appl. Opt.*, vol. 15, pp. 1256–1259, 1976.

**Steven G. Matsik** received the B.S. degree from Wake Forest University, Winston-Salem, NC, in 1979 and the M.S. and Ph.D. degrees from Georgia State University (GSU), Atlanta, in 1996 and 1998, respectively.

His research has concentrated on development of semiconductor optoelectronic devices, and he has published more than 20 articles. He is currently with the Department of Physics and Astronomy, GSU.

Dr. Matsik was awarded the Outstanding Senior Graduate Student Award at GSU.

**Mohamed B. M. Rinzan** received the B.S. degree with First Class Honors in physics from the University of Kelaniya, Sri Lanka, in 1995, and the M.S. degree from Georgia State University (GSU), Atlanta, in 2003, where he is currently pursuing the Ph.D. degree.

His current research is on infrared detectors. He has also published seven papers.

Mr. Rinzan was awarded the Outstanding Advanced Graduate Student Award at GSU.

**Dmitriy G. Esaeu** received the M.S. degree from Novosibirsk State University, Russia, in 1974 and the Ph.D. degree from the Institute of Semiconductor Physics, Siberian Branch of the Russian Academy of Sciences, Russia in 1989.

His research interest is mainly in the field of investigation, design, characterization and simulation of IR detectors. He has authored more than 40 articles. He is currently with the Department of Physics and Astronomy, Georgia State University, Atlanta.

**A. G. Unil Perera** (SM'97) received the B.S. degree with First Class Honors in physics from the University of Colombo, Sri Lanka in 1981 and the M.S. and Ph.D. degrees from the University of Pittsburgh, Pittsburgh, PA in 1983 and 1987, respectively.

Until 1992, he was a Research Assistant Professor at the University of Pittsburgh. In 1992, he joined Georgia State University, Atlanta, where he is currently a Full Professor. His research embraces development of semiconductor optoelectronic devices ranging from biology to electronics, as well as the search for fractional charge impurities (quarks) in semiconductors. He is the Director of the Interaction of Radiation with Matter Laboratory (IRML) and is a member of the Center for Neural Communication and Computation and also the Graduate Director of Physics. He has published five book chapters and more than 80 research articles and has a patent on infrared detectors.

Dr. Perera won the Outstanding Science Student of the Year Award at the University of Colombo, and was awarded the 1995 Junior Faculty Award and the 1999 Faculty Achievement Award at Georgia State University. He is a member of APS and SPIE.

**G. von Winckel** received the B.S.E.E. degree in electrical engineering from the University of Connecticut, Storrs, in 1998 and the M.S.E.E. in electrical engineering from the University of Connecticut in 2000. He is currently pursuing the Ph.D. degree in electrical and computer engineering and the M.S. degree in applied mathematics at the University of New Mexico, Albuquerque.

His present research interests include growth and modeling of semiconductor nanostructures.

**Andreas Stintz** was born in Merseburg, Germany, in 1964. He received the Ph.D. degree in physics from the University of New Mexico, Albuquerque, in 1993. The subject of his thesis was field desorption phenomena.

From 1994 to 1995, he was a Postdoctoral Fellow at the Department of Physics and Astronomy at the University of New Mexico, where he investigated the singlet D resonance in the H-ion. In 1996, he joined the Center for High Technology Materials and became involved in crystal growth of III-V semiconductors by molecular-beam epitaxy. His research includes high-power quantum well lasers, quantum dot lasers and detectors, saturable absorbers and crystal growth on metamorphic buffer layers. He also co-founded Zia Laser, Inc., in 2000, a startup company with the goal of marketing a new generation of telecom and datacom lasers.

**Sanjay Krishna** received the M.S. degree in physics from the Indian Institute of Technology (IIT), Madras, India, in 1996 and the M.S. degree in electrical engineering and the Ph.D. degree in applied physics from the University of Michigan, Ann Arbor, in 1999 and 2001, respectively.

He is an Assistant Professor of Electrical and Computer Engineering at the Center for High Technology Materials, University of New Mexico. His present research interests include growth, fabrication, and characterization of self-assembled quantum dots and type-II InAs-InGaSb-based strain layer superlattices for mid-infrared lasers and detectors. In his research group, studies are also undertaken on carrier dynamics and relaxation mechanisms in quasi-0 dimensional systems and the manipulation of these favorable relaxation times to realize high temperature mid infrared detectors. He has authored or coauthored more than 25 peer-reviewed journal articles, over 20 conference presentations, and two book chapters.

Dr. Krishna received the Gold Medal from the IIT in 1996 for the best academic performance in the Masters program in physics. He is also the Vice-chair of the local IEEE/LEOS chapter.

**H. C. Liu** received the Ph.D. degree in applied physics from the University of Pittsburgh, Pittsburgh, PA, in 1987.

He is currently the Principal Research Officer and is the Quantum Devices Group Leader in the Institute for Microstructural Sciences at the National Research Council of Canada, Ottawa, ON. He has authored and coauthored approximately 237 papers, has given presentations at approximately 52 invited conferences, and has been granted 10 patents.

**M. D. Byloos**, photograph and biography not available at the time of publication.

**T. Oogarah**, photograph and biography not available at the time of publication.

**G. I. Sproule**, photograph and biography not available at the time of publication.

**K. Liu**, photograph and biography not available at the time of publication.

**M. Buchanan**, photograph and biography not available at the time of publication.